Research in Molecular Medicine

Designing Anticancer Peptides Based on Diphtheria Toxin, CRM197 and HB-EGF-like Growth Factor Interactions

Soheila Ghaderi[1], **Shirin Tarahomjoo**[2*]

1. Department of Central Laboratory, Razi Vaccine and Serum Research Institute, Agricultural Research, Education and Extension Organization (AREEO), Karaj, Iran.
2. Department of Antigen Studies, Razi Vaccine and Serum Research Institute, Agricultural Research, Education and Extension Organization (AREEO), Karaj, Iran.

Use your device to scan and read the article online

Citation Ghaderi S, Tarahomjoo Sh. Designing Anticancer Peptides Based on Diphtheria Toxin, CRM197 and HB-EGF-like Growth Factor Interactions. Research in Molecular Medicine. 2025; 13(2):131-140. https://doi.org/10.32598/rmm.13.2.1441.2

https://doi.org/10.32598/rmm.13.2.1441.2

Article Type:
Research Paper

Article info:
Received: 07 Feb 2025
Revised: 24 Feb 2025
Accepted: 15 Apr 2025

Keywords:
Anti-cancer peptides, Diphtheria toxin (DT), Epidermal growth factor receptor (EGFR), Heparin-binding epidermal growth factor-like growth factor (HB-EGF), Molecular dynamics (MD) simulations

ABSTRACT

Background: Diphtheria toxin (DT) and its non-toxic mutant, CRM197, possess anti-cancer properties. The membrane-anchored form of heparin-binding epidermal growth factor-like growth factor (HBEGF) is a cellular receptor for DT and CRM197. The R and T domains of DT and CRM197 are responsible for receptor binding and translocation of their catalytic domains to the cytosol, respectively. Moreover, HB-EGF is a ligand of the epidermal growth factor receptor (EGFR), which is involved in the signaling cascade for cancer progression. HB-EGF binds to EGFR at its EGF-like domain. This study aimed to design anti-cancer peptides based on interactions of DT and CRM197 with HB-EGF to inhibit the binding of HB-EGF to EGFR and thus prevent the signaling involved in cancer progression.

Materials and Methods: The DT-HB-EGF and the CRM197-HB-EGF complexes were analyzed using molecular dynamics (MD) simulations at 60 ns. The stability, allergenicity and antigenicity of peptides were assessed using Protparam, AlgPred, and Vaxijen softwares respectively.

Results: The root mean square fluctuation (RMSF) plots demonstrated that the amino acids of DT and CRM197 with lower fluctuations were located in the R and T domains. The Rg plots revealed that the structure of the DT-HB-EGF complex remained compact until 31 ns, after which its compactness decreased. The structure of CRM197-HB-EGF remained compact during simulations. The root mean square deviation (RMSD) plots indicated that the DT-HB-EGF complex remained stable for 31 ns. However, the CRM197-HB-EGF complex produced a stable trajectory during simulations. Assessing tertiary structures of the complexes showed that residues Ser508-Ser535 of DT (pDT) and Ser291-Tyr358 of CRM197 (pCRM) were bound to the EGF-like domain of HBEGF; therefore, these peptides can interfere with the binding of HB-EGF to EGFR. The pCRM peptide was located in the T domain of CRM197, while the pDT peptide was located within the R domain. The Protparam results showed that both peptides were stable. However, pCRM was more thermostable than pDT. None of the peptides was allergens, as revealed by AlgPred. The Vaxijen analysis demonstrated that pCRM was non-antigenic, whereas pDT was antigenic.

Conclusion: These results demonstrate the utility of pCRM as an anticancer peptide that inhibits HB-EGF binding to EGFR.

*** Corresponding Author:**
Shirin Tarahomjoo, PhD.
Address: *Department of Antigen Studies, Razi Vaccine and Serum Research Institute, Agricultural Research, Education and Extension Organization (AREEO), Karaj, Iran.*
Phone: *+98 (263) 4552194*
E-mail: *starahomjoo@gmail.com*

Research in Molecular Medicine

Introduction

Diphtheria toxin (DT) has been explored as a promising anticancer agent. The heparin-binding epidermal growth factor-like growth factor (HB-EGF) acts as the DT cellular receptor in its membrane-anchored form (HB-EGF precursor) [1, 2]. The DT structure consists of three domains, each with a specific biological function that supports its cytotoxic activity. The receptor-binding domain (R domain) comprising amino acids 386–535 of DT attaches to the cellular receptor and is located at the C-terminus of DT [3]. The transmembrane or translocation domain (T domain) of DT is essential for the transformation of the catalytic domain (C domain) into the cytosol, encompassing amino acid residues 205–378. The C-domain, comprising amino acids 1–185 of DT, catalyzes the NAD+-dependent ADP-ribosylation of eukaryotic elongation factor 2 (EF2), resulting in arrest of protein synthesis and thereby promoting cell apoptosis [4].

DT is one of the most studied bacterial toxins and has proven to be a convenient object for developing non-toxic mutants with defined features using protein engineering. These mutants are used in basic research and medical practice [5]. CRM197 is an enzymatically inactive, non-toxic mutant of DT that has undergone clinical trials for the treatment of ovarian cancers. However, it is an exogenous bacterial protein that induces immune responses in the host. Moreover, anti-DT antibodies cross-react with CRM197 and may thus neutralize its therapeutic activity [6, 7].

The R-domain of DT is composed of a β-barrel and mediates toxin binding to its receptor, the HB-EGF precursor [8, 9]. The binding of DT to the HB-EGF precursor triggers epidermal growth factor receptor (EGFR)-mediated endocytosis, directing the DT-HB-EGF complex to the endosomal pathway [10, 11].

HB-EGF is a member of the EGF family of EGFR ligands. In ovarian cancer, HB-EGF expression is increased in cancerous ovarian tissues compared to normal tissues and is linked to unfavorable clinical outcomes [12, 13]. Further studies have revealed that HB-EGF is involved in the initial response to chemotherapy and the development of chemotherapy resistance [14-16]. The EGF-like domain of HB-EGF, comprising amino acids 106-145 is essential for binding and activating EGFR [2, 17].

EGFR is a member of the ErbB family of tyrosine kinase receptors that transmits a growth-inducing signal to cells stimulated by an EGFR ligand [18, 19]. In normal tissues, the availability of EGFR ligands is tightly regulated to ensure that the kinetics of cell proliferation precisely match the tissue requirements for homeostasis. However, in cancer, EGFR is often perpetually stimulated because of the sustained production of EGFR ligands in the tumor microenvironment [20, 21] or by mutations that lock the receptor in a state of continuous activity [22]. The role of growth factor signaling in the pathogenesis of human cancers has long been established. EGFR is involved in the progression and pathogenesis of several human cancers. Inhibition of EGFR signaling pathways represents a promising therapeutic strategy for human cancers [23].

Therefore, this study aimed to design anti-cancer peptides that inhibit HB-EGF binding to EGFR to prevent the signaling cascade involved in cancer progression. To this end, the interactions of DT and CRM197 with HB-EGF were studied using molecular dynamics (MD) simulations. The results were analyzed using the root mean square fluctuation (RMSF), radius of gyration (Rg), and root mean square deviation (RMSD). The amino acid regions of DT and CRM197 critical for HB-EGF binding were determined. The physicochemical properties, such as allergenicity and antigenicity, of these peptides were assessed using bioinformatics tools. The results of this study are expected to be useful for the development of effective anticancer peptides with therapeutic activity against human cancers.

Materials and Methods

The DT and CRM197 structures were retrieved from the Protein Data Bank (RCSB PDB) using the PDB IDs 1XDT and 4AE0, respectively [24]. The protonation-fixing process was performed with DT and CRM197, prepared at pH 6.5 using the H++ server, which served as the input for MD simulations [25]. The stability of the DT structure at pH 6.5 was demonstrated in our previous study [26]. Therefore, the same pH was used in the current study. Protons were added to the input structure according to the calculated ionization states of the chemical groups at an intended pH. The output structure is in the PQR (PDB+charge+radius) format. Deep view (spdv3.7b2) was used to preview the files for missing side chains and to replace them with added OXT at the C-terminus. MD simulations were performed using the GROMACS 4.5.4 package with the AMBER99SB force field and periodic boundary conditions [27]. This study was conducted using the original Ubuntu 12.04 oper-

ating system, and the version of GROMACS deemed most appropriate for it was 4.5.5. The solute was then embedded in a TIP3P water box [28, 29]. Two distinct simulation boxes, DT-HB-EGF and CRM197-HB-EGF, were examined separately using GROMACS, and the intended analysis was performed. The simulation boxes were defined with dimensions of 10×10×10 nm for each structure. The boxes were then filled with the appropriate number of water molecules. To neutralize the system, appropriate numbers of sodium and chloride ions were added to each box. To eliminate any undesirable contact atoms and the initial kinetic energy in the simulation boxes, the energy was minimized by applying the steepest descent algorithm. Each of the defining systems was equilibrated in two stages: 5 ns NPT and NVT simulations with a pressure fixed at 1 bar. The temperature was set to 310 K in the simulations. To maintain a constant temperature, a velocity-rescaling thermostat was used [28]. To maintain constant pressure during the simulations, the Parrinello-Rahman barostat [30] was used in all equilibration steps and MD simulations. For each component of the system, PME algorithm [31] was applied to estimate the electrostatic interactions. The LINCS algorithm [32] was used to fix the chemical bonds in the protein atoms. Simulations of DT complexed with HB-EGF and CRM197 complexed with HB-EGF were performed at 60 ns and 310 K. The structures were visualized and analyzed using YASARA software. The average conformation of each model was extracted from the trajectory and compared with the initial model using the YASARA viewer and PyMol software. The secondary structure of CRM197 in the complex at intended regions was plotted using the poly view server.

Docking of DT and CRM197 to HB-EGF was performed using AutoDock 4.2, a widely used non-commercial docking program that effectively binds ligands to their target proteins, exhibiting both high accuracy and rapid computational performance [33]. The program was executed as an add-on to Chimera. The binding sites in DT were determined using the crystal structure of the DT-HB-EGF complex (PDB ID: 1XDT), and the HB-EGF structure was extracted from the complex structure. It was then attached to CRM197 in its PDB file (4AE0) to determine the binding sites of CRM197 to HB-EGF using the AutoDock protocol. Among all the possible poses suggested by AutoDock, the pose showing the maximum number of hydrogen bonds and the minimum binding free energy change (kcal/mol), as represented in the View Dock window, was selected. These were further analyzed in the Biovia Discovery Studio visualizer for the hydrogen bond formation between the functional groups of ligands and amino acids. Proteins were prepared by removing heteroatoms and adding hydrogens and charges. For Docking of HB-EGF to the chemical ligand (CHEMBL3288258), the simulation interactions diagram (103928613 of PubChem- Binding DB-External ID: 50017345) was converted to a PDB file using Biovia Discovery Studio, followed by peptide docking in AutoDock. For this purpose, PDBQT format files for the target and ligand were prepared using their PDB files. Moreover, Grid and Docking parameters files (a.gpf and a.dpf) were provided. Molecular docking was performed using Cygwin. The results were analyzed, and the minimum binding free energy change (kcal/mol) of the complex, as represented in the View Dock window, was selected.

The physicochemical properties of the peptides were determined using the ProtParam program [34]. The antigenicity of the peptides was evaluated using Vaxijen software [35]. The allergenicity of the peptides was assessed using AlgPred software [36].

Results

The fluctuations of amino acid residues in the DT complexed with HB-EGF and CRM197 complexed with HB-EGF were analyzed using the RMSF plot (Figure 1). Lower fluctuations and, hence, lower flexibilities were observed in the DT amino acids, including Leu304, Leu346, Ile364, Thr400, Asp417, Thr436, Met459, Gly480, Ser501, Ser508, Phe530, and Ser535, within the DT-HB-EGF complex (Figure 1). In addition, the CRM197 amino acids comprising Phe250, Ser291, Thr300, Val340, Tyr358, Trp398, Ala430, Cys471, His484, Ile499, and Ile504, and Phe530 showed lower fluctuations within the CRM197-HB-EGF complex. Figure 2 shows the Rg plots of the DT-HB-EGF and CRM197-HB-EGF complexes during the MD simulations. The Rg value of the DT-HB-EGF complex increased from 2.89 nm at the beginning of the simulation to 2.76 nm at 31 ns. It increased to 5.5 nm at 32 ns and further increased to 7.2 nm at the end of the simulation (60 ns).

The Rg value of the CRM197-HB-EGF complex increased from 2.89 nm at the start of the simulation to 3.31 nm at the end of the simulation. The RMSD profiles of the complexes were derived from 60 ns MD simulations (Figure 3). The RMSD value of the DT-HB-EGF complex at 31 ns of the simulation was 1.00 nm, while it reached 3.94 nm at 32 ns and further increased to 5.83 nm at the end of the simulation (60 ns). The RMSD value of the CRM197-HB-EGF complex reached 1.52 nm at the end of the simulation. Given that changes in the conformational stability of the DT-HB-EGF complex were observed at 30 ns, an addition-

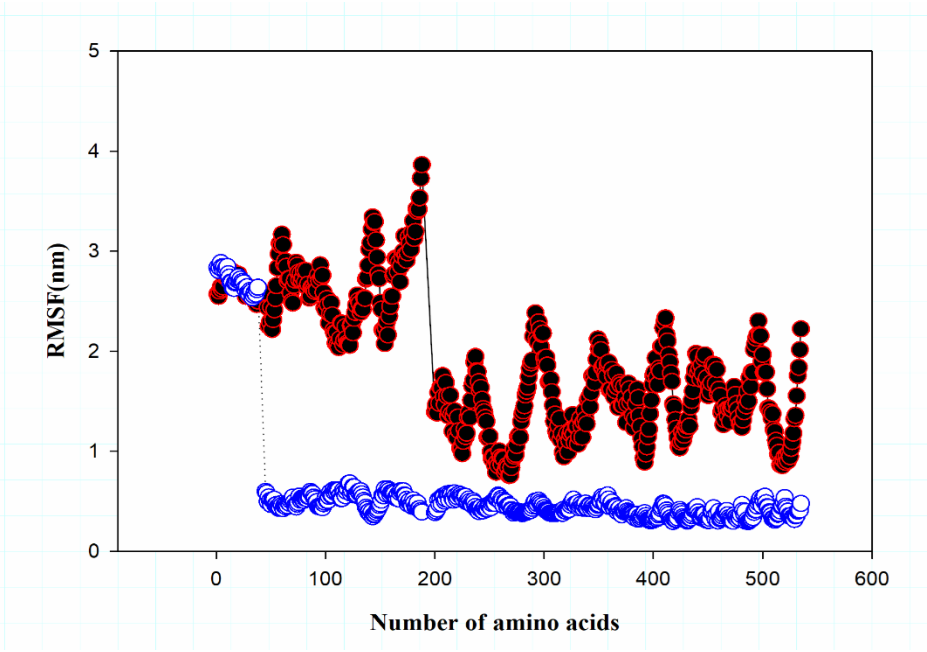

Figure 1. The RMSF plots of DT-HB-EGF and CRM197-HB-EGF complexes following 60ns MD simulations

Note: The RMSF values of the CRM197-HB-EGF complex were shown by open blue circles. The RMSF values of the DT-HB-EGF complex were indicated by filled red circles.

al 30 ns was added to ensure the structure's stability and confirm the correctness of the results. However, the conformational stability of the CRM197-HB-EGF complex was maintained during the simulation. We assessed the tertiary structure of the DT-HB-EGF complex using YASARA software (Figure 4A). The residues Ser508-Ser535 of DT and Pro107-Ser147 of HB-EGF comprised the key amino acid regions involved in the complex formation between DT and HB-EGF. Moreover, the amino acids Ser291-Tyr358 of CRM197 and Pro107-Ser147 of HB-EGF were the key amino acid regions responsible for complexing CRM197 and HB-EGF (Figure 4B). Assessing the secondary structure of pCRM in the CRM197-HBEGF complex (Figure 5) revealed that the amino acid residues Leu297-Ser305 and Ile310-Met314 were located in α-helix. In contrast, the residues Ile316-Ala317 and Ala320-Val321 were located in β-sheets, indicating intramolecular hydrogen bond formation and hence the stability of the peptide structure. The binding energy of the pCRM-HB-EGF complex was compared with that of the HB-EGF-CL complex. The ΔG value of the pCRM-HB-EGF complex (0.0215 kcal/mol) was significantly lower than that of HB-EGFCL (182 kcal/mol). These results indicated that the binding stability of pCRM to HB-EGF was much higher than that of CL to HB-EGF. Figure 6 shows the secondary structure of pCRM. It consists of α-helix, coils, and β-sheets, which contribute to

Table 1. Physicochemical properties of peptides determined by protparam

Physicochemical Properties	pDT	pCRM
II	-3.67	27.85
Half-life in mammalian cells	1.9 h	1.9 h
Half-life in *E. coli*	>10 h	>10 h
Half-life in Yeast	>20 h	>20 h
AI	100.71	122.06
GRAVY score	-0.032	0.631

Abbreviations: pDT: Peptides derived from diphtheria toxin; GRAVY: Grand average of hydropathicity; AI: Aliphatic index.

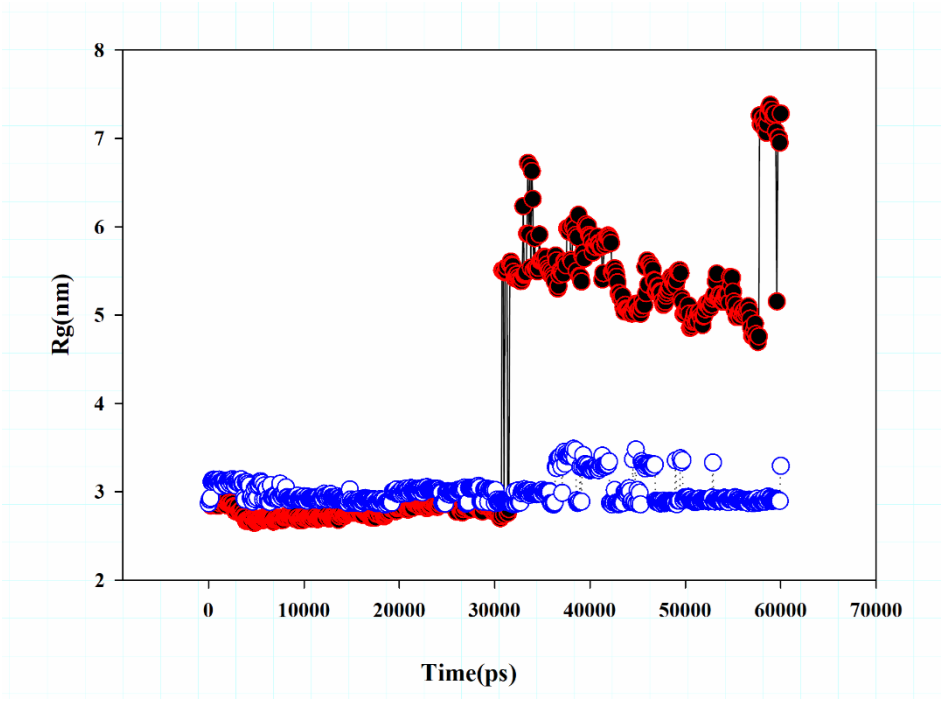

Figure 2. The Rg plots of DT-HB-EGF and CRM197-HB-EGF complexes during 60ns MD simulations

Note: The Rg values of the CRM197-HB-EGF complex were shown by open blue circles. The Rg values of the DT-HB-EGF complex were indicated by filled red circles.

peptide stability through hydrogen bonding. The physico-chemical properties of the peptides derived from DT (pDT) and CRM197 (pCRM) were analyzed by Protparam (Table 1). The estimated half-lives of the peptides in mammalian cells, Escherichia coli, and yeast were 1.9h, >10 h, and >20h, respectively. The AI of pCRM was higher than that of pDT. The GRAVY score of pDT was lower than that of pCRM. Furthermore, we assessed the allergenicity and antigenicity of the peptides using Algpred and VaxiJen software (Table 2). Our results indicated that none of the peptides were allergens. Moreover, pCRM197 was not antigenic, whereas pDT was antigenic.

Discussion

The RMSF values determined during MD simulations demonstrate the average atomic mobility of the backbone atoms (N, Cα, and C) relative to their average positions, thereby capturing the flexibility of individual amino acid residues. A high RMSF value indicates greater flexibility of the amino acid residue, whereas a low RMSF value indicates lower flexibility of the amino acid residue [37]. The amino acids involved in the interaction between DT and HB-EGF were determined in our study considering the amino acids with lower fluctuations in the RMSF plot (Figure 1). Moreover, we determined the amino acids of CRM197implicated in the interaction of CRM197 and HB-EGF. These amino acids showed lower fluctuations in the RMSF plot of the CRM197-HB-EGF complex (Figure 1). The identified amino acids showing lower fluctuations in DT and CRM197 were located within the R and T domains. The molecular spatial packing of amino acid residues is a crucial aspect of protein stability. Compact packing of amino acid residues is known to establish both the stability and folding rate of proteins. Rg provides information about the size and compactness of proteins. The struc- tural changes in proteins during MD simulations were quantified using Rg values [38, 39]. The Rg plot of the DT-HB-EGF complex indicated

Table 2. Allergenicity and antigenicity of peptides determined by algpred and vaxijen

Peptides	Allergenicity (Algpred)	Antigenicity (VaxiJen)
pDT	Non-allergen	Antigen
pCRM	Non-allergen	Non-antigen

pDT: Peptides derived from diphtheria toxin.

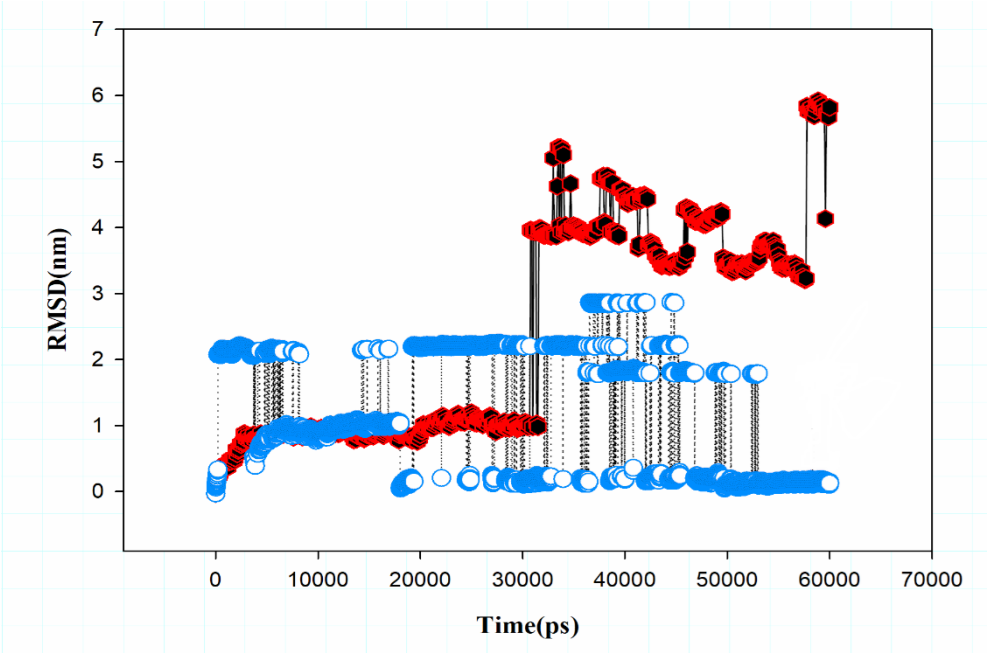

Figure 3. The RMSD plots of DT-HB-EGF and CRM197-HB-EGF complexes during 60ns MD simulations

Note: The RMSD values of the CRM197-HB-EGF complex were shown by open blue circles. The RMSD values of the DT-HB-EGF complex were indicated by filled red circles.

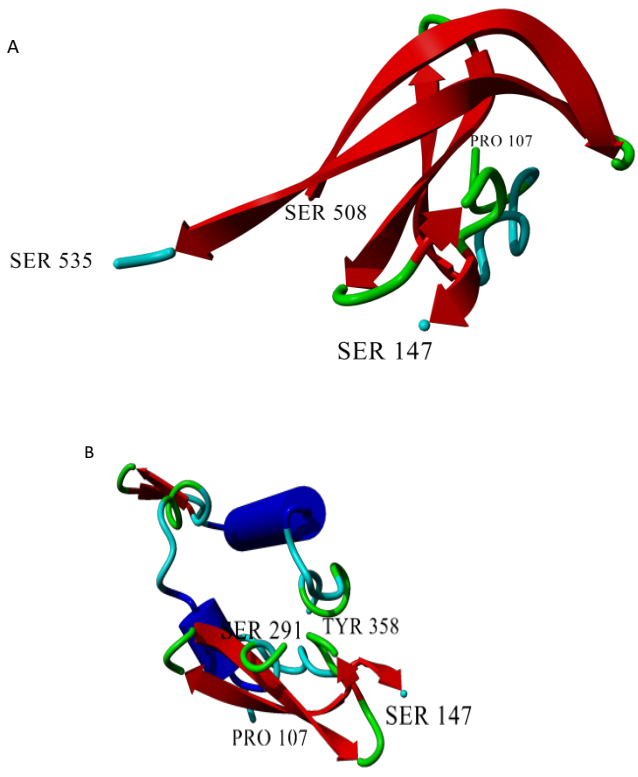

Figure 4. A) The three-dimensional structure snapshot of DT-HB-EGF complex showing residues Ser508-Ser535 of DT after 60 ns MD simulations, B) The tertiary structure snapshot of the CRM197-HB-EGF complex showing residues Ser291-Tyr358 of CRM197

Note: The tertiary structures of HB-EGF at residues Pro107-Ser147 were demonstrated in the figures.

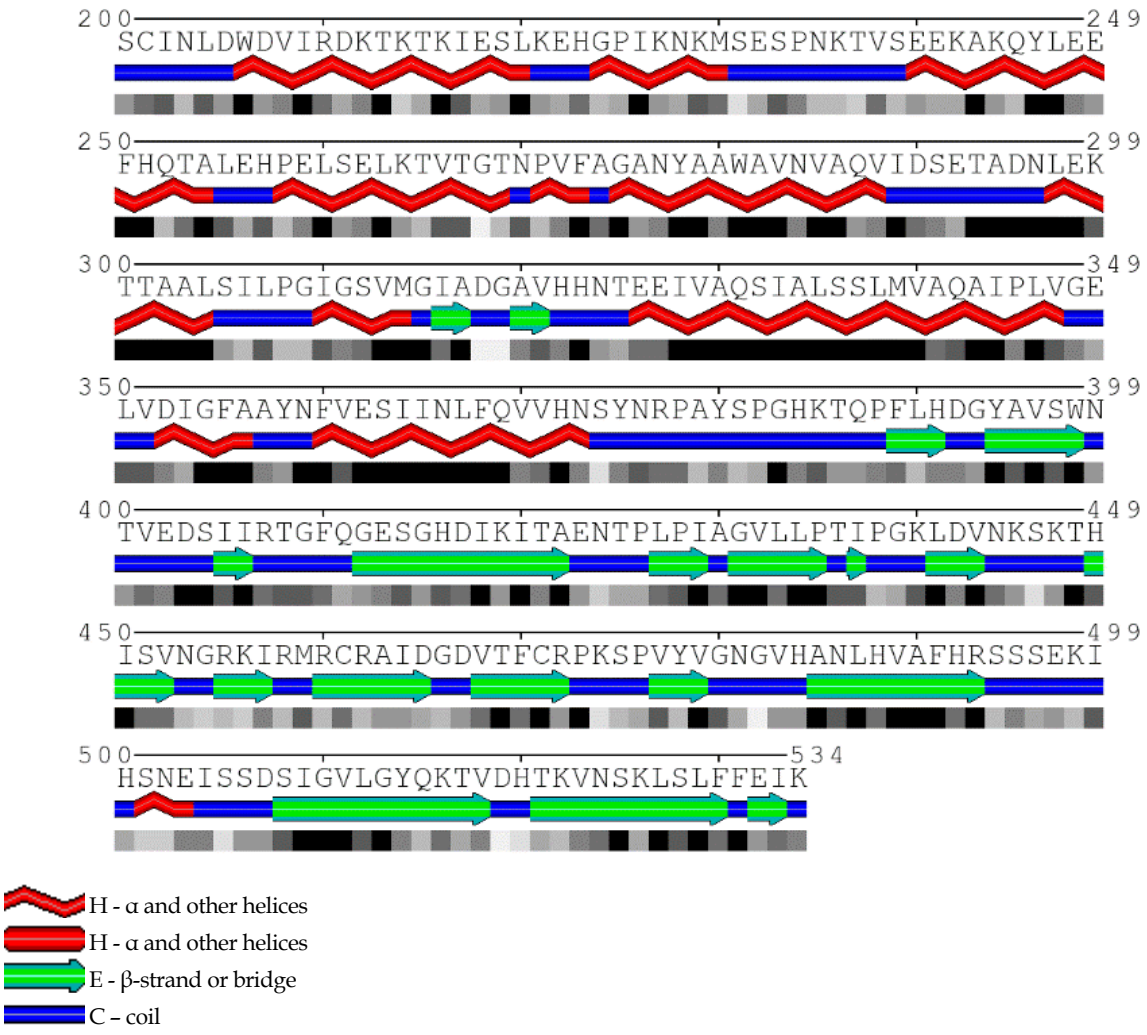

Figure 5. The secondary structure of the CRM197-HB-EGF complex at chain B of CRM197 including pCRM after 60ns of simulations derived from poly view server

that the complex structure was compact until 31 ns (Figure 2). However, the compactness decreased from 32 to 60 ns. The structure of CRM197-HB-EGF complex remained compact during the simulation. RMSD is a key parameter for analyzing the equilibration of MD trajectories. The RMSD values of the protein backbone atoms were plotted against time to evaluate the stability of each system during the simulations [40].

The RMSD profile of the DT-HB-EGF complex indicated the complex stability until 31 ns of the simulation. However, the complex stability decreased from 32 to 60 ns. Moreover, the RMSD plot of the CRM197-HB-EGF complex demonstrated that the simulation produced a stable trajectory. The analysis of RMSD and Rg demonstrated the conformational stability of the CRM197-HB-EGF complex, and the lower fluctuations observed in the RMSF plot of this complex indicated the binding stability of CRM197 to HB-EGF. However, assessing RMSD and Rg for the DT-HB-EGF complex revealed its conformational instability, and higher fluctuations in its RMSF plot indicated the unstable binding of DT to HB-EGF. The EGF-like domain of HB-EGF mediates its binding to EGFR, resulting in EGFR activation. This domain comprises amino acid residues 106-145 of HB-EGF [2, 17].

The key amino acid region of DT mediating the complex formation with HB-EGF was located within the R-domain and composed of β-sheets (Figure 4A). The key amino acid region of CRM197 involved in the complex formation with HB-EGF resided on the T-domain and was composed of α-helix, β-sheets, and coils (Figure 4B). The mutation of glycine 52 of DT to glutamic acid in CRM197 induces structural changes in the C- domain and the solvent accessibility of the R-domain [41]. Our

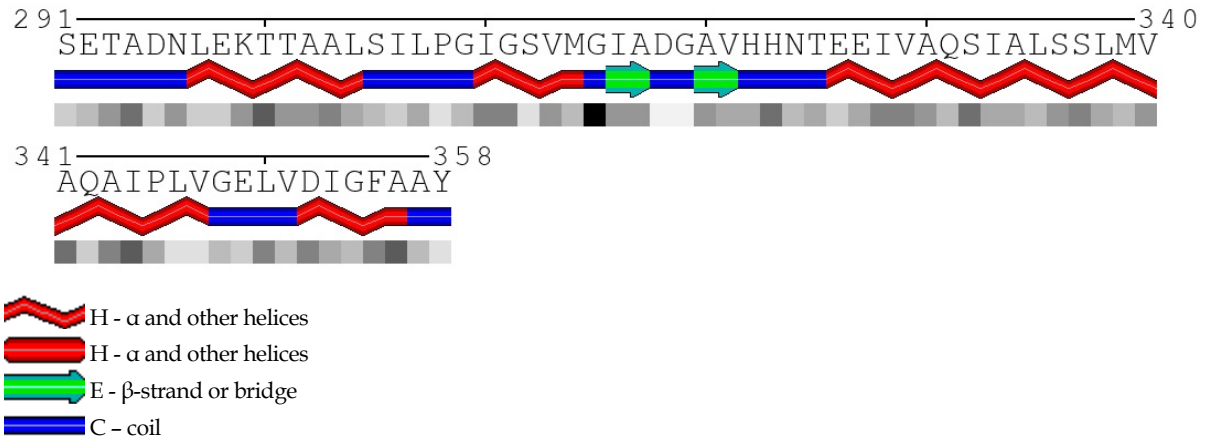

Figure 6. The secondary structure of pCRM

analysis also demonstrated differences in the binding regions of DT and CRM197 for the EGF-like domain of HB-EGF. The construction and analysis of chimeric and mutant forms of the HB-EGF precursor showed the importance of residues E141, R115, and L127 for the functioning of the HB-EGF precursor as a DT-receptor [42, 43]. These amino acids were included in the key amino acid regions of HB-EGF (Pro107-Ser147) identified in this study. The key amino acid regions of DT and CRM197 were bound to amino acids Pro107-Ser147 of HB-EGF, situated in its EGF-like domain (residues 106-145). Therefore, peptides targeting key amino acid regions can interfere with binding to EGFR and inhibit downstream signaling pathways responsible for cancer progression.

The instability index (II) is a measure of peptide stability; values less than 40 indicate stable peptides [34]. The II values of pCRM and pDT were less than 40, implying their stability. The peptide half life was dependent on the nature of the amino-terminus residues according to the N-end rule [34]. Similar half-lives were predicted for the peptides in different hosts. The aliphatic index (AI) is a positive correlate of thermostability, and the grand average of hydropathicity (GRAVY) score is an indicator of hydropathicity [34]. The AI analysis showed that pCRM was more thermostable than pDT. The GRAVY scores indicate that pDT interacts more strongly with water molecules than pCRM. Allergenicity analysis revealed non-allergenicity of these peptides. Non-antigenicity was shown for pCRM, whereas pDT was antigenic. These results imply the usefulness of pCRM as an anticancer peptide that inhibits the binding of HB-EGF to EGR, thereby blocking the signaling pathway involved in cancer promotion.

Conclusion

In this study, we assessed the interactions between DT and CRM197 with HB-EGF using MD simulations, analyzing RMSF, Rg, and RMSD. Our results demonstrated that amino acid residues Ser508-Ser535 of DT and Ser291-Tyr358 of CRM197 constitute the critical amino acid regions of these proteins involved in the formation of a complex with HB-EGF through the EGF-like domain of HB-EGF. These peptides can interfere with HB-EGF binding to EGFR and thus abolish the subsequent signaling pathway responsible for cancer promotion. Therefore, these peptides may have anticancer properties. These peptides were non-allergenic. The CRM197-derived peptide was non-antigenic; hence, using this peptide as an anticancer agent is advantageous over the DT-derived peptide. Moreover, the peptide derived from CRM197 mapped to the T-domain, indicating the role of this domain in inhibiting HB-EGF function in tumor growth and progression.

Ethical Considerations

Compliance with ethical guidelines

There were no ethical considerations to be considered in this research.

Funding

This research did not receive any grant from funding agencies in the public, commercial, or non-profit sectors.

Authors contribution's

Conceptualization: Soheila Ghaderi; Review & editing: Shirin Tarahomjoo; Methodology, investigation, supervision and Writing the original draft: All authors.

Conflict of interest

The authors declared no conflicts of interest.

References

[1] Buzzi S. Diphtheria toxin treatment of human advanced cancer. Cancer Res. 1982; 42(5):2054-8. [Link]

[2] Mitamura T, Higashiyama S, Taniguchi N, Klagsbrun M, Mekada E. Diphtheria toxin binds to the epidermal growth factor (EGF)-like domain of human heparin-binding EGF-like growth factor/diphtheria toxin receptor and inhibits specifically its mitogenic activity. J Biol Chem. 1995; 270(3):1015-9. [DOI:10.1074/jbc.270.3.1015] [PMID]

[3] Rolf JM, Gaudin HM, Eidels L. Localization of the diphtheria toxin receptor-binding domain to the carboxyl-terminal Mr approximately 6000 region of the toxin. J Biol Chem. 1990; 265(13):7331-7. [DOI:10.1016/S0021-9258(19)39118-5] [PMID]

[4] Menestrina G, Schiavo G, Montecucco C. Molecular mechanisms of action of bacterial protein toxins. Mol Aspects Med. 1994; 15(2):79-193. [DOI:10.1016/0098-2997(94)90043-4] [PMID]

[5] Romaniuk SI, Kolibo DB, Komisarenko SV. [Perspectives of application of recombinant diphtheria toxin derivatives (Russian)]. Bioorg Khim. 2012; 38(6):639-52. [DOI:10.1134/S106816201206012X] [PMID]

[6] Rappuoli R. New and improved vaccines against diphtheria and tetanus. N Gener Vaccines. 1997; 417-35. [Link]

[7] Suzuki K, Mizushima H, Abe H, Iwamoto R, Nakamura H, Mekada E. Identification of diphtheria toxin R domain mutants with enhanced inhibitory activity against HB-EGF. J Biochem. 2015; 157(5):331-43. [DOI:10.1093/jb/mvu079] [PMID]

[8] Iwamoto R, Senoh H, Okada Y, Uchida T, Mekada E. An antibody that inhibits the binding of diphtheria toxin to cells revealed the association of a 27-kDa membrane protein with the diphtheria toxin receptor. J Biol Chem. 1991; 266(30):20463-9. [DOI:10.1016/S0021-9258(18)54947-4] [PMID]

[9] Naglich JG, Metherall JE, Russell DW, Eidels L. Expression cloning of a diphtheria toxin receptor: Identity with a heparin-binding EGF-like growth factor precursor. Cell. 1992; 69(6):1051-61. [DOI:10.1016/0092-8674(92)90623-K] [PMID]

[10] Dorland RB, Middlebrook JL, Leppla SH. Receptor-mediated internalization and degradation of diphtheria toxin by monkey kidney cells. J Biol Chem. 1979; 254(22):11337-42. [DOI:10.1016/S0021-9258(19)86490-6] [PMID]

[11] Morris R, Gerstein A, Bonventre P, Saelinger C. Receptor-mediated entry of diphtheria toxin into monkey kidney (Vero) cells: Electron microscopic evaluation. Infect Immun. 1985; 50(3):721-7. [DOI:10.1128/iai.50.3.721-727.1985] [PMID] [PMCID]

[12] Miyamoto S, Hirata M, Yamazaki A, Kageyama T, Hasuwa H, Mizushima H, et al. Heparin-binding EGF-like growth factor is a promising target for ovarian cancer therapy. Cancer Res. 2004; 64(16):5720-7. [DOI:10.1158/0008-5472.CAN-04-0811] [PMID]

[13] Tanaka Y, Miyamoto S, Suzuki SO, Oki E, Yagi H, Sonoda K, et al. Clinical significance of heparin-binding epidermal growth factor-like growth factor and a disintegrin and metalloprotease 17 expression in human ovarian cancer. Clin Cancer Res. 2005; 11(13):4783-92. [DOI:10.1158/1078-0432.CCR-04-1426] [PMID]

[14] Wang F, Liu R, Lee S, Sloss C, Couget J, Cusack J. Heparin-binding EGF-like growth factor is an early response gene to chemotherapy and contributes to chemotherapy resistance. Oncogene. 2007; 26(14):2006-16. [DOI:10.1038/sj.onc.1209999] [PMID]

[15] Sanui A, Yotsumoto F, Tsujioka H, Fukami T, Horiuchi S, Shirota K, et al. HB-EGF inhibition in combination with various anticancer agents enhances its antitumor effects in gastric cancer. Anticancer Res. 2010; 30(8):3143-9. [Link]

[16] Yagi H, Yotsumoto F, Sonoda K, Kuroki M, Mekada E, Miyamoto S. Synergistic anti-tumor effect of paclitaxel with CRM197, an inhibitor of HB-EGF, in ovarian cancer. Int J Cancer. 2009; 124(6):1429-39. [DOI:10.1002/ijc.24031] [PMID]

[17] Higashiyama S, Lau K, Besner G, Abraham JA, Klagsbrun M. Structure of heparin-binding EGF-like growth factor. Multiple forms, primary structure, and glycosylation of the mature protein. J Biol Che. 1992; 267(9):6205-12. [DOI:10.1016/S0021-9258(18)42682-8] [PMID]

[18] Carpenter G, Cohen S. Epidermal growth factor. J Biol Chem. 1990; 265(14):7709-12. [DOI:10.1016/S0021-9258(19)38983-5] [PMID]

[19] Alroy I, Yarden Y. The ErbB signaling network in embryogenesis and oncogenesis: Signal diversification through combinatorial ligand-receptor interactions. FEBS Lett. 1997; 410(1):83-6. [DOI:10.1016/S0014-5793(97)00412-2] [PMID]

[20] Hynes NE, Lane HA. ERBB receptors and cancer: The complexity of targeted inhibitors. Nat Rev Cancer. 2005; 5(5):341-54. [DOI:10.1038/nrc1609] [PMID]

[21] Mendelsohn J, Baselga J. The EGF receptor family as targets for cancer therapy. Oncogene. 2000; 19(56):6550-65. [DOI:10.1038/sj.onc.1204082] [PMID]

[22] Wong AJ, Ruppert JM, Bigner SH, Grzeschik CH, Humphrey PA, Bigner DS, et al. Structural alterations of the epidermal growth factor receptor gene in human gliomas. Proceed Natl Acad Sci. 1992; 89(7):2965-9. [DOI:10.1073/pnas.89.7.2965] [PMID] [PMCID]

[23] Hirata A, Ogawa S-i, Kometani T, Kuwano T, Naito S, Kuwano M, et al. ZD1839 (Iressa) induces antiangiogenic effects through inhibition of epidermal growth factor receptor tyrosine kinase. Cancer Res. 2002; 62(9):2554-60. [Link]

[24] Louie GV, Yang W, Bowman ME, Choe S. Crystal structure of the complex of diphtheria toxin with an extracellular fragment of its receptor. Mol Cell. 1997; 1(1):67-78. [DOI:10.1016/S1097-2765(00)80008-8] [PMID]

[25] Hess B, Kutzner C, Van Der Spoel D, Lindahl E. GROMACS 4: Algorithms for highly efficient, load-balanced, and scalable molecular simulation. J Chem Theory Comput. 2008; 4(3):435-47. [DOI:10.1021/ct700301q] [PMID] [PMCID]

[26] Ghaderi S, Bozorgmehr MR, Morsali A. Structure study and predict the function of the diphtheria toxin in different pH levels (Acidic-Basic-Natural) using molecular dynamics simulations. Entomol Appl Sci Lett. 2016; 3(4-2016):49-56. [Link]

[27] Satpathy R, Guru RK, Behera R, Priyadarshini A. Homology modelling of lycopene cleavage oxygenase: The key enzyme of bixin production. J Comput Sci Syst Biol. 2010; 3(3):59-63. [DOI:10.4172/jcsb.1000057]

[28] Jorgensen WL, Chandrasekhar J, Madura JD, Impey RW, Klein ML. Comparison of simple potential functions for simulating liquid water. J Chem Physics. 1983; 79(2):926-35. [DOI:10.1063/1.445869]

[29] Bussi G, Donadio D, Parrinello M. Canonical sampling through velocity rescaling. J Chem Physics. 2007; 126(1):014101. [DOI:10.1063/1.2408420] [PMID]

[30] Parrinello M, Rahman A, Vashishta P. Structural transitions in superionic conductors. Phys Rev Lett. 1983; 50(14):1073. [DOI:10.1103/PhysRevLett.50.1073]

[31] Darden T, York D, Pedersen L. Particle mesh Ewald: An N log (N) method for Ewald sums in large systems. J Chem Phys. 1993; 98(12):10089-92. [DOI:10.1063/1.464397]

[32] Hess B, Bekker H, Berendsen HJ, Fraaije JG. LINCS: A linear constraint solver for molecular simulations. Journal Of Comput Chem. 1997; 18(12):1463-72. [DOI:10.1002/(SICI)1096-987X(199709)18:123.0.CO;2-H]

[33] Forli S, Olson AJ. A force field with discrete displaceable waters and desolvation entropy for hydrated ligand docking. J Med Chem. 2012; 55(2):623-38. [DOI:10.1021/jm2005145] [PMID] [PMCID]

[34] Wilkins MR, Gasteiger E, Bairoch A, Sanchez JC, Williams KL, Appel RD, et al. Protein identification and analysis tools in the ExPASy server. Methods Mol Biol. 1999; 112:531-52. [DOI:10.1385/1-59259-584-7:531] [PMID] [PMCID]

[35] Doytchinova IA, Flower DR. Bioinformatic approach for identifying parasite and fungal candidate subunit vaccines. Open Vaccine J. 2008; 1(1):4. [DOI:10.2174/1875035400801010022]

[36] Saha S, Raghava GP. AlgPred: Prediction of allergenic proteins and mapping of IgE epitopes. Nucleic Acids Res. 2006; 34(Web Server issue):W202-9. [DOI:10.1093/nar/gkl343] [PMID] [PMCID]

[37] Falconi M, Biocca S, Novelli G, Desideri A. Molecular dynamics simulation of human LOX-1 provides an explanation for the lack of OxLDL binding to the Trp150Ala mutant. BMC structural biology. 2007; 7(1):73. [DOI:10.1186/1472-6807-7-73] [PMID] [PMCID]

[38] Makarov DE, Keller CA, Plaxco KW, Metiu H. How the folding rate constant of simple, single-domain proteins depends on the number of native contacts. Proceed Natl Acad Sci. 2002; 99(6):3535-9. [DOI:10.1073/pnas.052713599] [PMID] [PMCID]

[39] Tsai CJ, Nussinov R. Hydrophobic folding units at protein-protein interfaces: Implications to protein folding and to protein-protein association. Protein Sci. 1997; 6(7):1426-37. [DOI:10.1002/pro.5560060707] [PMID] [PMCID]

[40] Kumar A, Purohit R. Computational centrosomics: An approach to understand the dynamic behaviour of centrosome. Gene. 2012; 511(1):125-6. [DOI:10.1016/j.gene.2012.09.040] [PMID]

[41] Briday M, Carvalho N, Oganesyan N, Chang MJ, Lees A, Brier S, Chenal A. Comparative analysis of the structural dynamics of diphtheria toxin and CRM197 carrier proteins used in the development of conjugate vaccines. Int J Pharm. 2025; 675:125535. [DOI:10.1016/j.ijpharm.2025.125535] [PMID]

[42] Hooper KP, Eidels L. Glutamic acid 141 of the diphtheria toxin receptor (HB-EGF precursor) is critical for toxin binding and toxin sensitivity. Biochem Biophys Res Commun. 1996; 220(3):675-80. [DOI:10.1006/bbrc.1996.0463] [PMID]

[43] Mitamura T, Umata T, Nakano F, Shishido Y, Toyoda T, Itai A, et al. Structure-function analysis of the diphtheria toxin receptor toxin binding site by site-directed mutagenesis. J Biol Chem. 1997; 272(43):27084-90. [DOI:10.1074/jbc.272.43.27084] [PMID]